Danie G. Poolman,[1] *B. Eng. and P. Chris Pistorius,*[2] *Ph.D.*

The Possibility of Using Elemental Analysis to Identify Debris from the Cutting of Mild Steel

REFERENCE: Poolman DG, Pistorius PC. The possibility of using elemental analysis to identify debris from the cutting of mild steel. J Forensic Sci 1996;41(6):998–1004.

ABSTRACT: The debris produced by abrasive and oxygen-acetylene cutting of mild steel has been examined by scanning electron microscopy, energy-dispersive X-ray analysis, inductively coupled plasma atomic emission spectrometry, and X-ray diffraction, to establish which of these techniques are useful to test whether debris originated from a given source. Because of its poor sensitivity to trace amounts of elements, energy-dispersive X-ray analysis cannot be used for this purpose. However, when analyzed by inductively coupled plasma atomic emission spectrometry, the line intensities from chromium, nickel, cadmium, zinc, and copper in debris were mostly within 30% of the intensities for the source of the debris (with the intensities expressed relative to that from manganese). It was found that the morphology of the debris (as studied by scanning electron microscopy) did not give an unambiguous indication of the cutting technique, although X-ray diffraction did reveal that the debris from oxygen-acetylene cutting was oxidized to a greater degree than that from abrasive cutting.

KEYWORDS: forensic science, criminalistics, metal debris, trace elements, inductively coupled plasma atomic emission spectrometry

The cutting of mild steel, a ubiquitous material of construction, appears to be a common operation during the commission of certain crimes (for example, safe-breaking); cutting is normally effected by means of an oxygen-acetylene cutting torch, or a portable abrasive grinder, or both simultaneously (1). The debris produced by these cutting operations potentially provides a valuable forensic tool by testing whether the debris found on a suspect is related to debris found at the scene of the crime, or to the source of the debris (such as the original steel or parent material itself). This paper discusses techniques that may be useful for examining such debris. To serve a forensic purpose, a technique should meet at least two requirements. First, it must be sensitive to subtle differences in the composition of the parent material (most commonly mild steel) that was cut; second, it must be able to link debris to the parent material, despite the expected changes in composition because of oxidation (burning) of the debris during cutting.

Previous approaches to examining such debris included examination in a scanning electron microscope with energy dispersive X-ray analysis (SEM/EDX), and identification of phases by X-ray diffraction (XRD) (1–3). It was stated that the presence of nonspherical particles in the cutting debris indicated that a grinder, rather than a cutting torch, had been used (2). A related problem identifying different metal sections of a burnt-out vehicle was approached by using spectroscopic techniques (4) to determine both the presence and the concentration of elements.

Mild steel is a simple iron-based alloy, primarily containing a small amount of carbon (typically around 0.1 w/o) and manganese (typically around 0.5 w/o). Hence, differentiating different compositions of mild steel requires a technique that can detect and quantify trace elements in the steel. Inductively coupled plasma atomic emission spectroscopy (ICP-AES) has been used for this purpose for metal and glass sections (5–12). The work reported here examined the use of SEM examination, EDX, X-ray diffraction, and ICP-AES to identify the type of cutting operation, to detect trace element differences among different batches of mild steel, and to link debris to a specific source.

Experimental Work

Specimen Preparation: Cutting

Two mild steel rods (labeled A and B), each 6 m long and 12 mm in diameter, were used to provide the starting material for cutting trials. The chemical composition of the two rods is given

TABLE 1—*Chemical composition of the two mild steel rods used in this investigation. The compositions were determined by optical emission spectrometry and are given in weight percent. Accuracy is better than 0.001% for all elements except Mn, for which the accuracy is better than 0.01%. Samples were not analyzed for cadmium or zinc.*

Elements	Rod A	Rod B
C	0.029	0.166
Mn	0.34	0.71
P	0.006	0.022
S	0.013	0.048
Si	0.007	0.196
Ni	0.017	0.018
Cu	0.008	0.011
Cr	0.011	0.040
Mo	<0.001	0.003
V	0.001	0.002
Al	0.007	0.012
Ti	0.001	0.001
Nb	0.004	0.003
W	0.005	0.004
Zr	0.001	0.002
Co	0.004	0.004

[1]Forensic analyst, Forensic Science Laboratory, Private Bag X620, 0001 Pretoria, and Department of Materials Science and Metallurgical Engineering, University of Pretoria, 0002 Pretoria, South Africa.

[2]Associate professor, Department of Materials Science and Metallurgical Engineering, University of Pretoria, South Africa.

Received for publication 4 Aug. 1995; revised manuscript received 20 Oct. 1995 and 28 Feb. 1996; accepted for publication 18 March 1996.

TABLE 2—*Summary of cutting procedures applied to the different bars. The original rod (A or B) from which each bar had been taken is also indicated.*

Bar no.	Rod	Cutting procedure
1	A	Oxygen-acetylene cutting, high flame temperature
2	A	Oxygen-acetylene cutting, lower flame temperature
6	A	Oxygen-acetylene cutting, lower flame temperature and oxygen blasting
10	B	Grinding: performance disk
12	A	Grinding: INOX disk
13	A	Grinding: standard disk
19	B	Grinding: concrete disk
14	B	Grinding: standard disk, distance effect
15	A	Grinding: performance disk, distance effect
16	B	Grinding: INOX disk, distance effect

in Table 1. The 6-m long rods were cut to 0.5-m lengths (which are referred to as bars in this paper). To cut the bars to length, a fixed abrasive disk cutter was used at one end of each bar, and an oxygen-acetylene torch at the other. The bars were numbered from 1 to 24, and was each subjected to a different cutting technique as indicated in Table 2. Before cutting, specimens were drilled from the bars, with a specimen being taken 5 mm from each end, as well as at the middle of the bar. During the subsequent cutting operation, stainless steel trays were used in most cases to collect the debris. In the case of abrasive cutting, the trays extended up to 3 m from the cutting area. In three cases (debris from bars number 14, 15, and 16—see Table 2), possible distance effects were examined by collecting the debris in four different trays. These trays respectively extended 0 to 540 mm, 540 to 1080 mm, 1080 to 1620 mm, and 1620 to 2800 mm from the cutting area. The distance effect was not considered for oxygen-acetylene cutting because the debris is inherently spread over a smaller area for this cutting method. The debris from bar number 2 was not collected in a tray, but was swept from the concrete floor below the cutting area to evaluate possible contamination effects.

Although well over 900 types of abrasive disks are available locally, these were narrowed down to four basic types with the help of a representative of a local distributor.[3] These four types are as follows:

(1) Standard product: Used for most kinds of steel,
(2) Performance product: Also used for most kinds of steel, but with a different binder that is said to impart a longer life,
(3) INOX: Used for stainless steel, and
(4) Concrete: Used for concrete and brick.

Only one disk diameter was used because the distributor stated[3] that the many combinations of disk diameter and rotation rate all serve to provide approximately the same tangential speed (80 m/s) at the outer diameter of the cutting disk. In this work, the disk diameter was 230 mm and the rotation speed 6500 rpm (giving a tangential speed of 78.3 m/s).

Sample Preparation:

Examination and Analysis

ICP-AES Analysis—Before ICP-AES analysis, the samples were magnetically separated to reduce contamination by extraneous particles (including material from the grinder disk). Magnetic separation was performed manually in the following manner. The debris was placed in a watch-glass, and holding a bar magnet beneath the debris, the watch glass was inverted, allowing nonmagnetic particles to drop into a second watch glass. This process was repeated (on average 17 times) until no particles visibly fell upon inversion of the watch glass. The X-ray diffraction results that are presented later in this paper show the major components of the debris to be metallic iron, magnetite (Fe_3O_4), and wüstite (FeO); these phases are assumed to be present in each particle together with the trace elements (in oxidized or metallic form). Of these phases, metallic iron and magnetite are magnetic allowing the debris particles to be separated from possible contaminating particles. Clearly, this technique is only useful for magnetic debris, but based on the X-ray diffraction results, the debris from the cutting of most types of steel is expected to contain sufficient magnetite or metallic iron to allow magnetic separation to be used. In the practical examination of debris that was gathered from clothing (not further reported in this paper), it was not attempted to use magnetic separation to remove the debris from the clothing. Rather, the clothing was shaken out over stainless steel trays and magnetic separation was then applied to the contents of these trays.

For the quantification of the ICP-AES results, the concentration ratio method of analysis (5) was used here. The intensity of the line from each element was expressed relative to that from manganese (being the most abundant alloying element in mild steel). This method obviates the need for accurate weighing of the initial sample and accurate measurement of the final volume. However, in this project, accuracy of sample preparation was used as well because (as shown below) some effect of sample weight was found. Each sample was weighed to 0.18 ± 0.02 g. A volume of 40-mL analytical grade HCl was used to dissolve each sample in a quartz beaker. The samples were left to digest for 24 h and then prepared for analysis by adding 30 mL of demineralized water to the sample solution. This constant matrix of 40-mL HCl and 30-mL H_2O was maintained throughout the project to minimize drifting due to matrix fluctuation. Four subsamples were prepared from each sample, and each of these subsamples analyzed by ICP-AES. The elements that were analyzed are given in Table 3 together with wavelengths that were chosen; these wavelengths minimize interference from Fe (13).

A test of the effect of sample mass on ICP-AES analysis was used to decide on the standard mass of 0.18 g. In this test, drillings from bar number 8 were used to prepare ten samples with masses ranging from 0.02 to 0.189 g. Apart from the different masses, the preparation procedure was as given above. The resulting relative intensities are reported in Fig. 1; evidently, reliable results require a sample mass of at least 0.09 g for the procedure and instrument that were used here. It was decided to use a mass of 0.18 g

[3]F. Huber, Pferd South Africa, personal communication.

TABLE 3—*Elements analyzed by ICP-AES with the spectral lines used for analysis.*

Element	Mn	Si	Cr	Ni	Cd	Zn	S	Al	Cu
λ (nm)	257.61	251.611	283.563	231.604	226.502	213.856	180.731	396.152	324.754

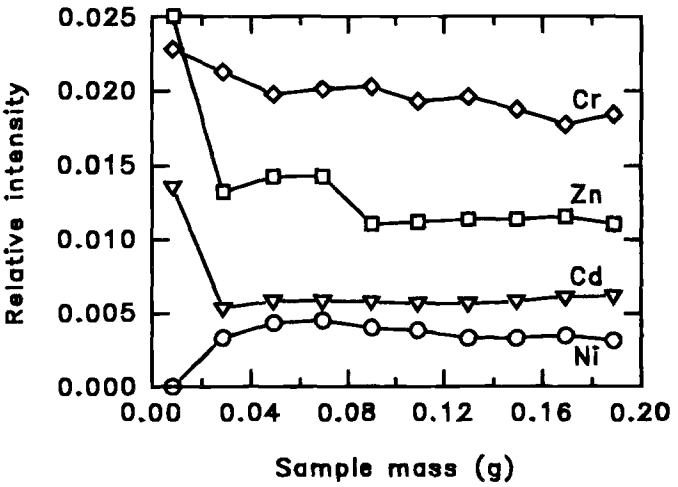

FIG. 1—*Effect of sample mass on the intensities from four elements (relative to manganese), for drillings of Rod B as analyzed by ICP-AES.*

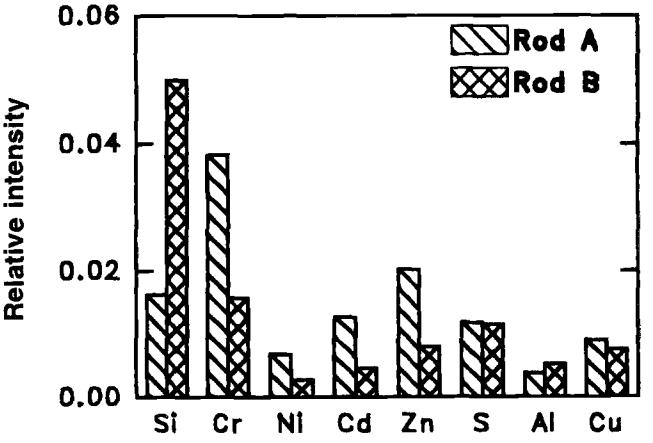

FIG. 3—*Comparison of the results from ICP-AES analysis of the two mild steel rods (A and B) used to produced cutting debris. Element intensities are expressed relative to that from Mn.*

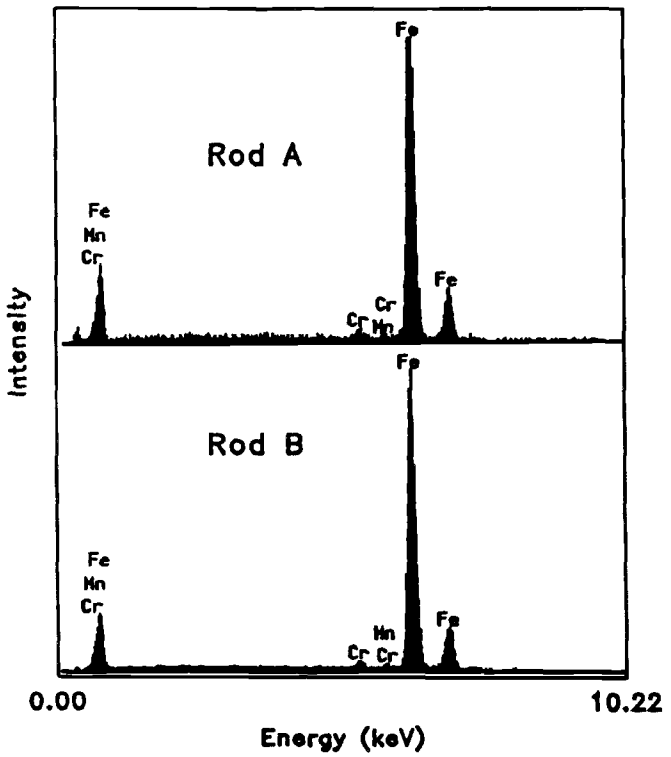

FIG. 2—*Spectra from energy-dispersive X-ray analysis of the two mild steel rods (A and B) from which cutting debris was produced.*

per sample because sufficient material was available. Practical experience showed that the mass of particles collected in the pockets, shoes, rolled-up sleeves, and gloves of a person cutting through a mild steel barrier (such as the case of a safe) normally exceeds 5 g. Hence, the requirement of 0.09 g per sample can be met in practice.

X-ray Diffraction—An automated Siemens D501 X-ray diffractometer was used to perform qualitative analysis (phase identification). Cu K_α radiation was used (at 25 mA and 30 kV) with a secondary monochromator. The diffraction angle (2θ) was scanned from 10° to 80° at a rate of 3°/min. Iron fluorescence was treated by subtracting the background as noise. As external standard, calcium fluoride (CaF_2) was added to each sample in the mass ratio 1 to 4 (CaF_2 to sample). The mixed sample was powdered by means of a mortar and pestle before XRD analysis. Peaks were assigned using the JCPDS-ICDD PDF-2 database. The height of the two strongest peaks from each iron-containing phase (metallic iron, wüstite, magnetite, and hematite) was determined and expressed as a relative height using one CaF_2 peak as reference. The planar spacings of the crystal planes that gave rise to the relevant peaks are listed in Table 4.

Scanning Electron Microscopy—Samples were mounted on a copper stub by means of carbon dag and sputter coated with carbon. A working distance of 15 mm and an acceleration voltage of 20 kV were used.

TABLE 4—*Phases analyzed by X-ray diffraction with the planar spacings corresponding to the peaks used to detect each phase.*

Phase	Peak no.	Planar spacing (Å)
CaF_2	1	3.1550
Fe_3O_4	1	2.5320
(magnetite)	2	1.6158
FeO	1	2.1530
(wüstite)	2	2.4900
Fe_2O_3	1	2.5190
(hematite)	2	2.0779
Fe (α)	1	2.0268
(metallic iron)	2	1.4332

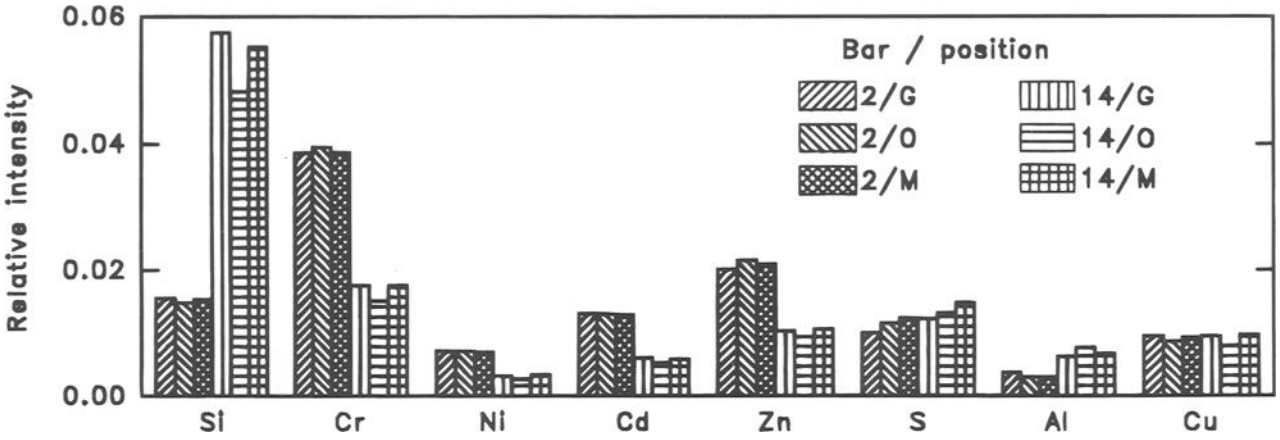

FIG. 4—*Reproducibility of ICP-AES analyses. The two graphs give the results for drillings taken from three positions on bars 2 and 14, which had been cut from rods A and B respectively. The position marked G was 5 mm from that end of each bar that had been abrasively cut, O was 5 mm from the other end, which had been cut by oxygen-acetylene, and M was midway between the two ends of the bar. Element intensities are expressed relative to that from Mn.*

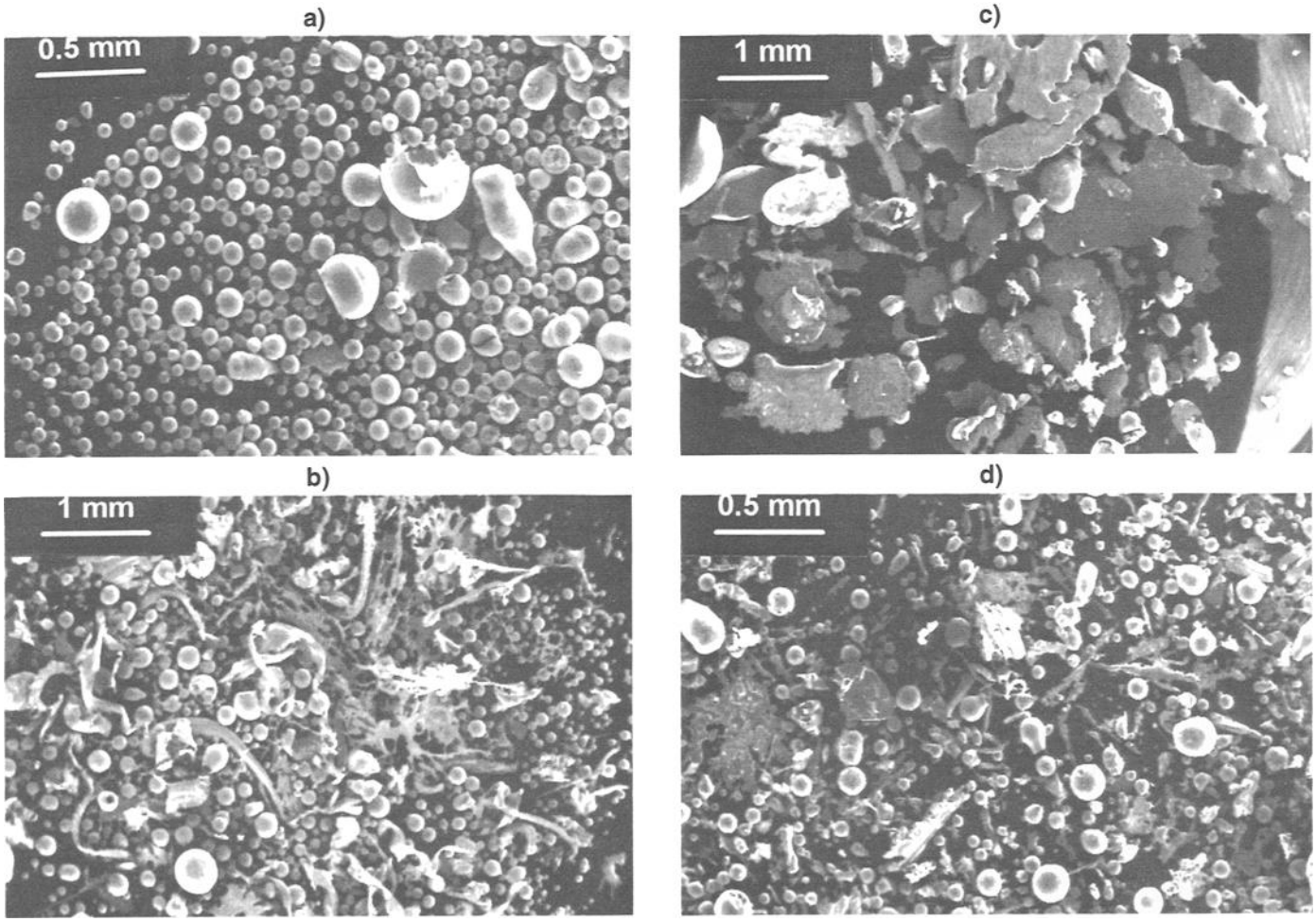

FIG. 5—*Scanning electron micrographs of cutting debris produced by different methods.* a) *Oxygen-acetylene cutting with high flame temperature;* b) *Grinding with INOX disk;* c) *Oxygen acetylene cutting with low flame temperature and oxygen blasting; and* d) *Grinding with standard disk.*

Results and Discussion

The compositions of the original two rods (A and B) were only slightly different; no significant compositional difference could be found by EDX, as illustrated in Fig. 2. Hence, EDX was not considered useful in this investigation and was not used further. Trace elements would have to be used to determine differences between different lots of nominally the same steel (mild steel in this case) to be able to trace debris to a specific source. ICP-AES successfully measures such differences: Fig. 3 gives relative peak heights (relative to that of Mn) for rods A and B. These can be seen to be clearly different. These differences are reproducible as illustrated by the results in Fig. 4, which show the analyses of drillings taken from three positions on bars 2 (from rod A) and 14 (from rod B). Thus, it appears that ICP-AES may be used to distinguish between different lots of the same type of steel. Clearly, general application of this approach would require a knowledge of the expected variations in trace element levels based on extensive sampling of different steel grades from different suppliers. Such sampling fell beyond the scope of the present work.

For the successful identification of debris by chemical analysis, it is also necessary to establish the relationship between the composition of the debris and that of its source. Establishing this relationship requires an understanding of the nature of the debris. To this end, the results of scanning electron microscopy and X-ray diffraction are presented first.

A range of particle morphologies and sizes was observed in the cutting debris. The previously reported preponderance of spherical particles in debris from oxygen-acetylene cutting and nonspherical particles in debris from abrasive cutting (2) was observed in some cases (Fig. 5a,b). However, nonspherical particles were common in the debris from oxygen-acetylene cutting with oxygen blasting (Fig. 5c), presumably because some particles had not solidified before hitting the collection tray; some debris from abrasive cutting contained mostly spherical particles (Fig. 5d). Clearly, microscopic examination of the debris may give some indication of the cutting method, but the results cannot be expected to be unambiguous.

The spherical form of many particles indicates heating above the melting point of the steel (approximately 1550°C). Exposure to high temperature in air is expected to cause at least partial oxidation. The X-ray diffraction results indicate that the iron in the debris from oxygen-acetylene cutting is fully oxidized (to FeO or Fe_3O_4), although some metallic iron is present in the debris from abrasive cutting (Fig. 6a). For the debris from abrasive cutting, there is a consistent trend of an increase in the magnetite peak heights with increasing distance from the cutting area and a decrease in the wüstite and iron peak heights (Fig. 6b). The decrease in wüstite peak height and the increased magnetite peak height may result from the eutectoid decomposition of wüstite to magnetite and iron, a reaction that becomes possible below 570°C (14). However, the associated decrease in the iron peak height indicates that it is more likely that the particles which were collected further from the cutting area were oxidized to a greater extent, presumably because these particles spent a longer time in flight.

The results from microscopical examination and X-ray diffraction thus indicate that the debris had been partially or fully molten, and that their iron component is fully or partially oxidized. Whether ICP-AES analysis would be successful or not in tracing debris to its metallic source depends on the extent to which trace elements are lost as a result of melting and oxidation. Trace elements may be lost through evaporation, either in the metallic form, or as a volatile oxide (for example, SO_2 or CrO_3).

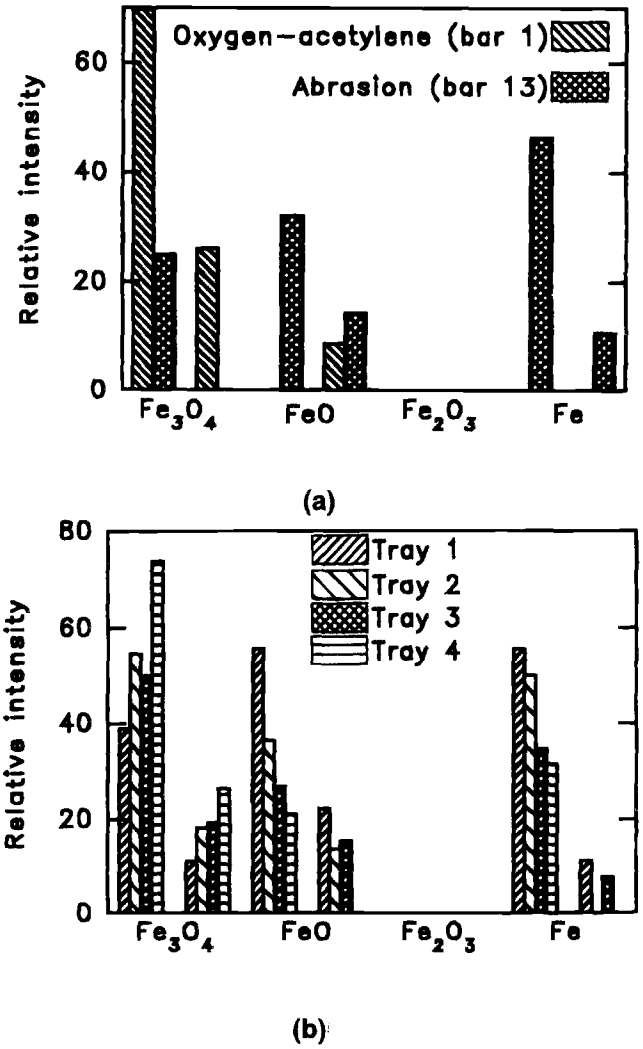

FIG. 6—*Peak heights from X-ray diffraction of cutting debris. The peak heights are normalized with respect to the CaF_2 peak.* a) *Comparison of the phases in debris produced by oxygen-acetylene cutting (debris from bar number 1) and abrasive grinding (debris from bar number 13).* b) *Change in phase distribution with distance from the cutting area for debris from grinding (debris from bar number 14). Tray 1 stretched from 0 to 540 mm from the cutting area, Tray 2 from 540 to 1080 mm, Tray 3 from 1080 to 1620 mm, and Tray 4 from 1620 to 2800 mm.*

A summary of the ICP-AES results is given in Fig. 7. As the legend indicates, the first seven bars at each element give the results for rod A and debris from cutting this rod in various ways (as detailed in Table 2), while the subsequent five bars at each element give the results for rod B and debris from cutting this rod. It is clear that the intensity (relative to manganese) obtained for the trace elements is affected by cutting. The intensities from silicon and aluminum are strongly affected and bear no consistent relation to the original values for the metal apart from being higher in almost all cases.

To decide reliably whether given debris originates from a given source, it is necessary to have a quantitative indication of the amount by which the relative intensities change as a result of cutting. A summary of the absolute values of the percentage changes in relative intensities is presented in Table 5; these values were calculated using the data presented in Fig. 7. The maximum and mean changes for each element are presented, grouped into the original rod type, and the cutting method. The changes are

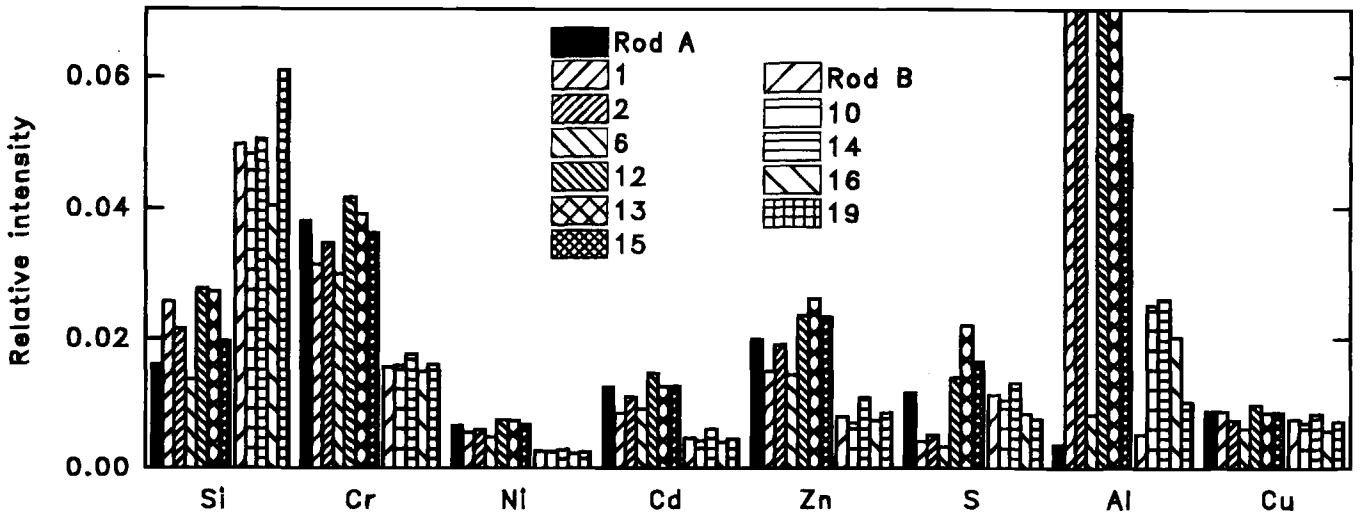

FIG. 7—*Summary of results of ICP-AES analysis of cutting debris together with the results for the original mild steel rods before cutting. Element intensities are expressed relative to that from Mn; relative intensities greater than 0.07 are truncated.*

TABLE 5—*Summary of the mean and maximum of the absolute values of the change in element intensity (expressed relative to the intensity from Mn) for debris produced by grinding or oxygen-acetylene cutting. The change is expressed as a percentage of the element intensities from drillings of the original rods that had been used to produce the cutting debris.*

	Rod A				Rod B	
	Ground		Oxygen-Acetylene		Ground	
	Max	Mean	Max	Mean	Max	Mean
Si	71	54	59	36	22	11
Cr	9	6	22	16	13	5
Ni	11	7	28	19	15	8
Cd	17	6	30	24	29	13
Zn	30	21	28	20	38	17
S	88	49	72	65	34	21
Al	4923	3162	7110	4150	400	292
Cu	9	6	32	17	24	12

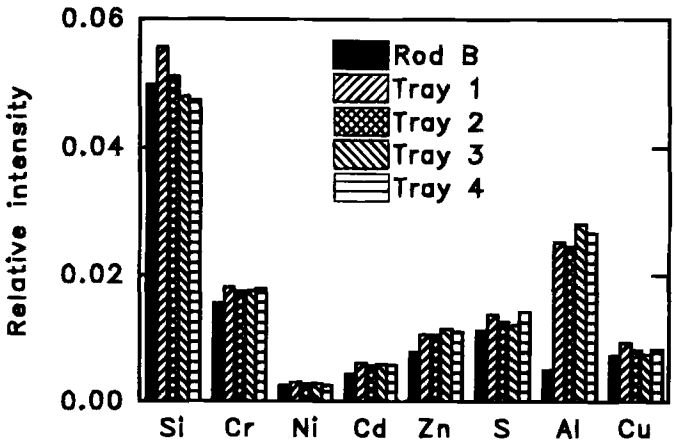

FIG. 8—*Results of ICP-AES analysis of grinding debris collected at different distances from the cutting area (debris from bar number 14). Tray 1 stretched from 0 to 540 mm from the cutting area, Tray 2 from 540 to 1080 mm, Tray 3 from 1080 to 1620 mm, and Tray 4 from 1620 to 2800 mm. Element intensities are expressed relative to that from Mn.*

referred to the average composition of respectively rods A and B. The average composition was calculated from the compositions of the individual test bars (which had been sampled in three places before cutting as mentioned above). It should be emphasized that the variations reported in Table 5 result from the different cutting techniques that had been used to obtain the debris; for samples from any one source, the variation in measured relative intensity was always less than 5% (see Figs. 4 and 8).

Table 5 emphasizes the large changes in the analyzed contents of aluminum and silicon in the debris relative to the source of the debris. Sulfur also shows large changes, which can be seen from Fig. 7 to be both increases (especially for debris from grinding) and decreases (for debris from oxygen-acetylene cutting). The increased sulfur content of the debris from bars 13 and 14, both of which had been ground with the standard disk, was found to originate from the binder of this disk. The sharp decrease of the sulfur content of the debris from oxygen-acetylene cutting (bars 1, 2, and 6) is probably related to the higher temperature and greater degree of oxidation, which promotes loss of sulfur by evaporation or as a gaseous oxide; this is also the probable reason for the sharp decreases in zinc, chromium, and cadmium of the debris from oxygen-acetylene cutting. The large increase in aluminum content (Fig. 7 and Table 5) may, in some cases, be due to contamination by abrasive particles (alumina) from the grinding disk. However, this cannot explain the increased aluminum content of the debris from oxygen-acetylene cutting nor the associated increase in silicon. The increases in aluminum and silicon *relative to manganese* may result from loss of manganese through evaporation allied with the formation of nonvolatile oxides by silicon and aluminum. It is worth noting that the debris, which had been intentionally contaminated by collection from a concrete floor rather than a stainless steel tray (debris from bar number 2), did not show larger increases in silicon or aluminum than any of the others (Fig. 7).

It can be concluded that analyzing for the elements chromium, nickel, cadmium, copper, and zinc is useful for establishing whether debris could have originated from a given source. With only two exceptions, the amount of these elements in the debris (relative to the manganese content) was within 30% of that in the original metallic source. The changes in silicon, aluminum, and sulfur

content appear too large to test whether such a relationship (between debris and a possible source) can exist. It would clearly depend on the compositions of the metals concerned whether this margin of 30% would be small enough to allow discrimination between possible source of debris, but the amounts of four of the elements mentioned above (Cr, Ni, Cd, and Zn) differed by more than 30% between the two mild steel rods used in this work (Fig. 3); these rods had been randomly selected at a steel vendor. This indicates that the trace element signature of different lots of mild steel may be sufficiently different to assign debris to specific sources, but further work is required to ascertain this. Such work would involve measuring the trace element composition of a range of steel grades from all the relevant suppliers; it may also be necessary to monitor changes in these compositions over time to allow for changes in steelmaking practices (for example, the level of scrap usage).

A possible relationship between debris which was found on the clothing of a suspect and the scene of a crime may also be tested by examining the trace element composition of not only the suspected metallic source of the debris, but also of debris found *at the scene of the crime.* Testing a relationship among various samples of debris requires knowledge of the amounts by which the trace element composition of debris from the same source can vary. Examination of Fig. 7 indicates that, as with the relationship between debris and its source, the amounts of respectively Cr, Ni, Cd, Zn, and Cu in debris produced by *different* cutting methods should mostly be within 30% of one another. For debris produced by a *single* cutting method, a spatial variation in composition may be expected because the degree of oxidation increases slightly with increased distance from the cutting area (Fig. 6b). Figure 8 shows this spatial variation to be small: this figure gives the trace element compositions for that debris, and its phase composition is presented in Fig. 6b. The results in Fig. 8 show that the spatial variation of the debris composition is less than 15% for Si, Cr, Cd, Zn, S, and Al and less than 20% for Ni and Cu, smaller than the differences with the composition of the source or of debris produced by other methods. Similar results were found for both other bars for which the distance effect was investigated. It was not attempted to compare the ICP-AES results with the original compositions as determined by optical emission spectrometry (Table 1), because the latter technique could only be used for the original solid metal and not for the debris particles.

Conclusion

Trace element analysis by ICP-AES is a promising way of distinguishing among different lots of the same steel type, and among debris originating from different sources. The debris produced by abrasive cutting and oxygen-acetylene cutting cannot always be distinguished on the basis of the presence of nonspherical particles, although the debris produced by the latter cutting method is more oxidized. Results from ICP-AES analysis indicate that the amounts of chromium, nickel, cadmium, zinc, and copper in the debris (expressed relative to the manganese content) match the amounts in the original metal and in debris produced from the same metal by other cutting methods to within 30% in almost all cases. Silicon, aluminum, and sulfur generally do not match. The spatial variation in the trace element composition of the debris is less than 20%.

References

(1) Collins B, Powell GLF. Identification of debris from the oxygen or abrasive cutting of safes. Scanning Electron Microsc 1979 (Pt 1):439–44.
(2) Zeichner A, Feingold G, Landau E. Abrasive cutting of a safe: A case study. J Forensic Sci 1993;38:1516–22.
(3) McDermott SD. Metal particles as evidence in criminal cases. J Forensic Sci 1993;39:1552–9.
(4) Powell GLF, Robinson RR. Trace element analysis of steel sections on either side of an oxygen cut in a vehicle suspected of being stolen. J Forensic Sci 1978;23:707–11.
(5) Ward AF, Marciello LF. Analysis of metal-alloys by inductively coupled argon plasma optical-emission spectrometry. Anal Chem 1979;51:2264–72.
(6) Locke J. The application of plasma source atomic emission spectrometry in forensic science. Anal Chim Acta 1980;113:3–12.
(7) Koons RD, Fiedler C, Rawalt RC. Classification and discrimination of sheet and container glasses by inductively coupled plasma-atomic emission-spectrometry and pattern-recognition. J Forensic Sci 1988;33:49–67.
(8) Koons RD, Peters CA, Rebbert PS. Comparison of refractive-index, energy-dispersive X-ray fluorescence and inductively coupled plasma atomic-emission spectrometry for forensic characterization of sheet glass fragments. J Anal At Spectrom 1991;6:451–6.
(9) Carpenter RC, Till C. Analysis of small samples of brasses by inductively coupled plasma-optical emission spectrometry and their classification by two pattern-recognition techniques. Analyst 1984;109:881–4.
(10) Koons RD, Peters CA, Merrill RA. Forensic comparison of household aluminum foils using elemental composition by inductively coupled plasma-atomic emission spectrometry. J Forensic Sci 1993;38:302–15.
(11) Powell GLF, Robinson RR, Cocks B, Wright M. Unlawful possession of silver. J Forensic Sci 1978;23:712–6.
(12) Vijayalakshmij S, Prabhu RK, Mahalingam TR, Mathews CK. Application of inductively coupled plasma-mass spectrometry in trace metal characterization of nuclear-materials. At Spectrosc 1992 March;13(2):61–6.
(13) Winge RK, Fassel VA, Peterson VJ, Floyd MA. Inductively coupled plasma-atomic emission spectroscopy—an atlas of spectral information, Fifth impression. Amsterdam: Elsevier, 1991.
(14) Schürmann E, Janhsen U. Determination of the phase boundaries of the wüstite solid solution within the context of reduction tests. Steel Res 1993;64:279–85.

Address request for reprints or additional information to
P. C. Pistorius
Department of Materials Science and Metallurgical Engineering
University of Pretoria
0002 Pretoria, South Africa